Characterization of a Buried Neutral Histidine in *Bacillus circulans* Xylanase: Internal Dynamics and Interaction with a Bound Water Molecule[†]

Gregory P. Connelly and Lawrence P. McIntosh*

Department of Biochemistry and Molecular Biology, Department of Chemistry, and the Protein Engineering Network of Centres of Excellence, University of British Columbia, Vancouver, British Columbia V6T 1Z3, Canada

ABSTRACT: NMR spectroscopy was used to characterize the dynamic behavior of His149 in *Bacillus circulans* xylanase (BCX) and its interaction with an internal water molecule. Rate constants for the specific acid- and base-catalyzed exchange following bimolecular kinetics (EX_2) of the nitrogen-bonded $H^{\epsilon 2}$ of this buried, neutral histidine were determined. At pD_{min} 7.0 and 30 °C, the lifetime for this proton is 9.9 h, corresponding to a protection factor of $\sim 10^7$ relative to that predicted for an exposed histidine. The apparent activation energies measured for specific acid and base catalysis (7.0 and 17.4 kcal/mol) indicate that exchange occurs via local structural fluctuations. Consistent with its buried environment, the $N^{\epsilon 2}-H$ bond vector of His149 shows restricted mobility, as evidenced by an order parameter $S^2 = 0.83$ determined from ^{15}N relaxation measurements. The crystal structure of BCX reveals that a conserved, buried water hydrogen-bonds to the $H^{\epsilon 2}$ of His149. Strong support for this interaction in solution is provided by the observation of a negative nuclear Overhauser effect (NOE) and positive rotating-frame Overhauser effect (ROE) between His149 $H^{\epsilon 2}$ and a water molecule with the same chemical shift as the bulk solvent. However, the chemical shift of $H^{\epsilon 2}$ (12.2 ppm) and a D/H fractionation factor close to unity (0.89 ± 0.02) indicate that this is not a so-called low-barrier hydrogen bond. Lower and upper bounds on the lifetime of the internal water are estimated to be 10^{-8} and 10^{-3} s. Therefore the chemical exchange of solvent protons with those of His149 $H^{\epsilon 2}$ and the diffusion or physical exchange of the internal water to which the histidine is hydrogen-bonded differ in rate by over 7 orders of magnitude.

The native structure of a protein is stabilized under physiological conditions by a delicate balance of entropic, hydrophobic, electrostatic, hydrogen-bonding, and van der Waals interactions. On an individual basis these interactions are comparable to thermal energies, and thus transient structural fluctuations, up to and including global unfolding, are constantly occurring in any ensemble of protein molecules. Understanding the contributions of this inherent flexibility toward the structure, stability, and functions of these molecules remains an important experimental and theoretical challenge. The dynamic behavior of proteins is amenable to study by a wide array of techniques, including nuclear magnetic resonance (NMR)[1] spectroscopy and hydrogen exchange (HX). While HX studies have typically

focused on the slowly exchanging main-chain amides in proteins, other labile groups can also provide structural and dynamic information. The side chains of histidine residues are one such example. Normally the nitrogen-bonded $H^{\delta 1}$ and $H^{\epsilon 2}$ of the imidazole ring exchange with the solvent too rapidly to be detected by standard NMR methods. However, when their exchange is slowed by burial within the core of a protein and/or by hydrogen bonding, measurement of their proton exchange rates can provide useful information about the local and global fluctuations that these macromolecules undergo.

Bacillus circulans xylanase (BCX) has emerged as a model β-glucanase with numerous potential applications in the food and pulp and paper industries. The enzyme has been characterized extensively in terms of its structure, stability, and enzymology (2−7). As part of these studies, we noted that BCX contains a buried histidine, His149, with its imidazole ring positioned by a complex network of hydrogen bonds involving the side chain of Ser130 and an internal water molecule,[2] as well as an aromatic-aromatic interaction with Tyr105 (Figure 1; 5). These residues are absolutely conserved in other members of the homologous, low molecular weight family G or 11 xylanases (10, 11). Furthermore, the bound water has been observed in all five members of this family for which crystallographic coordinates have

* Address correspondence to this author at the Department of Biochemistry and Molecular Biology, 2146 Health Sciences Mall, University of British Columbia, Vancouver, BC, Canada V6T 1Z3. Phone (604)-822-3341; e-mail mcintosh@otter.biochem.ubc.ca.

[1] Abbreviations: BCX, *Bacillus circulans* xylanase; BPTI, bovine pancreatic trypsin inhibitor; BSX, *Bacillus subtilis* xylanase; CSA, chemical shift anisotropy; acetate-d_3, ^{2}H-[2,2,2-^{2}H$_3$]acetate; DSS, sodium 2,2-dimethyl-2-silapentane-5-sulfonate; EX_2, exchange following bimolecular kinetics; HSQC, heteronuclear single quantum correlation spectroscopy; HX, hydrogen exchange; LBHB, low-barrier hydrogen bond; NMR, nuclear magnetic resonance; NOE, nuclear Overhauser effect; pH*, observed pH meter reading of a D_2O solution; pD, pH meter reading of a D_2O solution corrected for the glass electrode artifact (pD = pH* + 0.4; ref *1*); pD_{min}, pD where HX rate is a minimum; ROE, rotating-frame Overhauser effect.

[2] This internal water is W200 in the Brookhaven Protein Data Bank file 1XNB. Five additional waters are identified as buried in BCX using the program PRO_ACT (*8*).

been deposited in the Brookhaven Protein Data Bank[3] (*3*, *5*, *12*−*14*). Combined with the observation that mutation of His149 increases the susceptibility of BCX to irreversible thermal inactivation (*15*), this indicates that these conserved residues and the bound water molecule play an important role in stabilizing the structure of family G xylanases.

Previously, we have characterized the two histidines in BCX using NMR spectroscopy (*15*). Whereas the exposed His156 has a relatively unperturbed pK_a of ∼6.5, the buried His149 remains in the neutral $N^{\epsilon 2}H$ tautomeric form under all conditions examined. On the basis of the invariance of its ^{15}N and ^1H chemical shifts with decreasing pH at 30 °C, the pK_a of His149 was found to be <2.3. BCX unfolds at low pH, and thus His149 is never protonated significantly within the context of the native protein. Furthermore, the nitrogen-bonded $H^{\epsilon 2}$ of His149, detected at a chemical shift of 12.2 ppm, was found to exchange with D_2O with a lifetime of ∼7 h at pD 7.44 and 30 °C. This significant protection from solvent exchange must result from the inaccessibility of the imidazole ring and/or its hydrogen-bonding interactions.

To probe the structural and dynamic environment of this distinctive histidine residue and its interactions with a bound water molecule, we have extended these studies along three major avenues. First, we have characterized in detail the pH and temperature dependence of the hydrogen−deuterium exchange of His149 $H^{\epsilon 2}$, as well as the exchange of two protected tyrosine hydroxyls with unusually downfield-shifted H^{η} resonances. Second, we have used ^{15}N NMR relaxation measurements to study the motions of the imidazole ring of this residue. And third, we have investigated the bound water to which His149 is hydrogen-bonded using NOE and chemical shift measurements. Taken together, these studies demonstrate that His149 is held rigidly within the core of BCX and that its $H^{\epsilon 2}$ undergoes specific acid- and base-catalyzed EX_2 exchange with the solvent at a rate that is ∼10^7 times slower than predicted for an exposed, neutral histidine. This H−D exchange is significantly slower than the physical exchange of bulk water with the buried water molecule to which His149 is hydrogen-bonded.

MATERIALS AND METHODS

Protein Preparation. Samples of $^{13}C/^{15}N$-labeled, ^{15}N-labeled, and unlabeled xylanase were expressed in *Escherichia coli* strain 594 and purified by ion-exchange and size-exclusion chromatography, as described previously (*16*, *17*). Upon reexamination of the NMR spectra of these proteins, it was discovered that the $^{13}C/^{15}N$-labeled sample contained two mutations: Ser134 to Thr and Thr147 to Ser. The latter of these corresponds to that found in the homologous *Bacillus subtilis* xylanase (*16*), while the former substitution was introduced accidentally during subcloning of the gene encoding this xylanase. The two residues are located on the surface of the protein and the substitutions do not change its structure or enzymatic activity (*3*, *5*). NMR spectra of the wild-type and mutant forms of the enzyme are essentially identical, including resonances from His149 (G.P.C. and

[3] The Brookhaven Protein Data Bank codes are as follows: *Bacillus circulans* xylanase (1XNB), *Trichoderma harzianum* xylanase (1XND), *Trichoderma reesei* xylanase I (1XYN) and xylanase II (1XYO and 1XYP), and *Thermomyces lanuginosus* xylanase (1YNA).

L.P.M., unpublished results). For simplicity, these proteins will hereafter be referred to as BCX. All HX experiments and the D/H fractionation factor measurements were performed on the wild-type xylanase, while ^{15}N relaxation and studies of the bound water interactions were carried out using both the $^{13}C/^{15}N$-labeled mutant BCX and ^{15}N-labeled wild-type BCX. The $^{13}C/^{15}N$-labeled sample contained 0.8 mM protein in 25 mM acetate-d_3, 0.02% sodium azide, and 90% H_2O/10% D_2O at pH* 5.8. Specific conditions for the other samples are detailed in their respective sections below.

NMR Spectroscopy. NMR spectra were recorded with a Varian Unity spectrometer operating at 500 MHz for proton and equipped with a pulsed-field gradient $^1H/^{13}C/^{15}N$ probe. Data were processed using Felix v2.30 software (Biosym Inc., San Diego, CA), and assignments were taken from Plesniak et al. (*15*, *17*).

Hydrogen Exchange. Hydrogen exchange measurements were performed on unlabeled BCX under various conditions of pH, temperature, and buffer concentration. Aliquots (600 μL) of protein in 100% H_2O buffer were passed through 3 mL spin columns containing G-25 medium Sephadex. The gel beads were swollen overnight in 99.9% D_2O buffer at the desired pD. Each H_2O sample was titrated close to its target pH with microliter amounts of HCl or NaOH before being loaded onto the exchange column. Samples were spun at 6000 rpm for 2 min in a benchtop swinging-bucket centrifuge, immediately loaded into NMR tubes, and allowed to equilibrate in the magnet for ∼5 min prior to data acquisition. Unless stated otherwise, samples were 0.9 mM protein in 15 mM sodium acetate-d_3, 15 mM sodium phosphate, and 0.02% sodium azide. Each NMR data set for a given pD consisted of a time series of 1D spectra, individually acquired with 8−64 transients of 2K complex points over a spectral width of 10 kHz. Exchange was always followed to at least 90% completion, after which the pD of the sample was measured at room temperature. The small temperature dependencies of the pK_as of the buffers were not taken into account. The exchange rate k_{ex} was determined by fitting the height (I_t) of the $H^{\epsilon 2}$ peak versus time to the expression $I_t = I_0 \exp(-k_{ex}t) + I_\infty$, using KaleidaGraph (Synergy Software, Reading, PA). I_∞ accounts for the effect of residual HOD (∼5%). Errors in k_{ex} are estimated to be 5%, except at the highest and lowest pH*s, for which the errors are 10%. Exchange rates were measured in the same manner for the two tyrosine hydroxyl H^{η} protons with chemical shifts at 11.6 and 12.7 ppm.

^{15}N Relaxation Measurements. The T_1 and T_2 relaxation times and the steady-state ^1H−^{15}N NOE value for the $^{15}N^{\epsilon 2}$ of His149 in $^{13}C/^{15}N$-labeled BCX were measured and analyzed as described by Farrow et al. (*18*). Selective flip-back and cosine-modulated pulses were used to minimize the perturbation of the bulk water magnetization.

NOE/ROE Interactions of His149 $H^{\epsilon 2}$ with an Internal Water. ROE and NOE experiments were performed and analyzed on the $^{13}C/^{15}N$-labeled sample in the manner of Grzeseik and Bax (*19*). Since the signal from $H^{\epsilon 2}$ of His149 is well-resolved, the spectra were collected in 1D mode. The ^{13}C nuclei were exploited to eliminate possible intramolecular NOEs from protons with chemical shifts near that of water. Pertinent relaxation times (^{15}N T_1, ^1H−^{15}N T_{1ZZ}, and ^1H $T_{1\rho}$), as well as the steady-state levels of water magnetization, were measured in separate experiments using pulse sequences
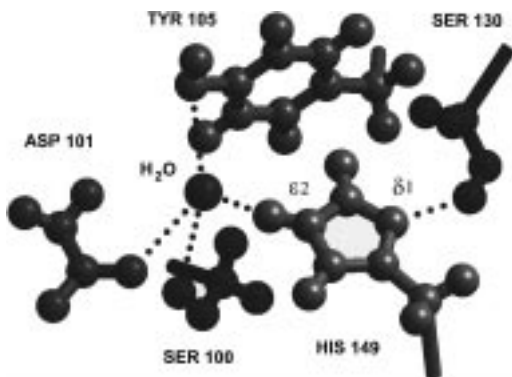
FIGURE 1: Environment of His149 in the crystal structure of BCX (5). His149 is hydrogen-bonded (dotted line) to the $O^\gamma H$ of Ser130 via its $N^{\delta 1}$ and to an internal water molecule via its $N^{\epsilon 2}H$. This water (W200 of the PDB file 1XNB) also interacts with the side chains of Ser100, Asp101, and Tyr105. Due to its buried, hydrogen-bonded environment, the labile $H^{\epsilon 2}$ of His149 exchanges with the solvent at a rate, ~10^7-fold slower than that predicted for an exposed imidazole ring. This figure was generated using the program SETOR (9).

provided by Dr. Lewis Kay (18, 20). These data were used to determine k_R and k_N, the rate constants for magnetization exchange between the $H^{\epsilon 2}$ proton of His149 and water protons during the ROE and NOE mixing periods, respectively.

Chemical Shift of the Bound Water. Gradient 11-echo $^1H-^1H$ NOESY spectra (21) were recorded on an unlabeled sample of BCX in the presence of 0, 2, 5, 10, and 30 mM $CoCl_2$. The protein was 0.8 mM in 10 mM sodium phosphate, 1 mM DSS, and 90% H_2O/10% D_2O at pH* 5.5. Aliquots of $CoCl_2$ were added from a 600 mM stock solution in 10 mM sodium phosphate. The sample pH* remained at 5.5 throughout the experiment. The increasing concentrations of Co^{2+} served to progressively change the chemical shift of bulk water, referenced to DSS at 0.00 ppm (22).

D/H Fractionation Factor. The D/H fractionation factor for the $H^{\epsilon 2}$ proton of His149 was determined by measuring the integral of its 1D ^1H NMR resonance at various solvent D_2O/H_2O ratios (23). Aliquots (60 μL) of a 4 mM stock solution of BCX in 100% H_2O were added to 600 μL of buffer solutions ranging from 10 to 100% D_2O. All samples were pH* 7.0 and contained 25 mM potassium phosphate. To ensure that the equilibrium ratio of D versus H was achieved, the samples were incubated for at least 3 exchange lifetimes at 30 °C. NMR spectra were recorded as 1024 transients of 2K complex points with a spectral width of 10 kHz. Normalized peak heights $I_{(x)}$ were plotted versus mole fraction of H_2O (x) and fit to the equation $I_{(x)} = x/[K_f (1 - x) + x]$, where K_f is the D/H fractionation factor (23). The extrapolated intensity of the $H^{\epsilon 2}$ proton signal in 100% H_2O was determined by reiteratively fitting the data to this expression.

RESULTS

Hydrogen−Deuterium Exchange of His149 $H^{\epsilon 2}$. The hydrogen-to-deuterium exchange rate of the $H^{\epsilon 2}$ of His149 was measured at 30 °C over a range of pD values from 4.60 to 9.50. Representative spectra can be found in Figure 6 of Plesniak et al. (15). A plot of the log k_{ex} versus pD has a V or chevron shape, indicative of both specific acid- and base-

catalyzed exchange (Figure 2a). At the pD_{min} = 7.0, the observed exchange rate k_{ex} is 2.8×10^{-5} s^{-1}, corresponding to a lifetime of 9.9 h. To obtain rate constants for catalysis by specific acid (k_A), specific base (k_B), and water (k_W), these data were fit to

$$k_{ex} = (k_A) \, 10^{-pD} + (k_B) \, 10^{(pD-pK_D)} + k_W$$

where the D_2O dissociation constant $K_D = 14.7$ at 30 °C (26, 27). The rate constants k_A, k_B, and k_W were determined to be 77 M^{-1} s^{-1}, 470 M^{-1} s^{-1}, and 1.1×10^{-5} s^{-1}, respectively, with fitting errors of ~10% for each rate constant. The data were also fit while the slopes of the acid and base limbs of the curve in Figure 2a were allowed to vary. The dependence of log k_{ex} upon pD and pOD remained close to first-order {d (log k_{ex})/d pD = 0.96 and d (log k_{ex})/d pOD = 0.89} and the rate constants k_A and k_B were within a factor of 3 of the above stated values.

The hydrogen-to-deuterium exchange of His149 $H^{\epsilon 2}$ was also monitored as a function of temperature over the range 10−40 °C, at both acidic (5.44) and basic (8.60) pD values relative to the pD_{min}. In Figure 2b the data are plotted as log k_{ex} versus 1/T. The slope of each line was used to calculate the apparent activation energies of exchange by specific acid (7.0 kcal mol^{-1}) and specific base catalysis (17.4 kcal mol^{-1}). The temperature dependence of K_D was neglected in this analysis, and thus the latter value also includes the enthalpy of ionization of D_2O (~14 kcal mol^{-1}; 28).

General acid catalysis by acetic acid was investigated with samples of BCX at pD 5.10 and 30 °C. The total ionic strength of each sample was held constant at 150 mM with the appropriate quantity of KCl, while the acetic acid concentrations studied were 5, 50, and 150 mM. The measured k_{ex} values were within 10% of 9.3×10^{-4} s^{-1} for all three samples, showing that the additional acetic acid had no effect on the exchange rate of His149 $H^{\epsilon 2}$. A small salt effect is seen, however, as the exchange rates of this proton in samples with ionic strengths of 0.5 and 0.15 M were 2- and 1.2-fold faster, respectively, than in 15 mM sodium acetate-d_3 and 15 mM sodium phosphate at pD 5.1. Under these acidic conditions, BCX carries a net positive charge as its theoretical pI is ~9.1. The small increase in exchange rate with increasing ionic strength is likely due to more effective screening of the overall electrostatic potential of the protein by the solvent counterions, thus allowing the positively charged exchange catalyst D$^+$ easier access to His149 (29).

^{15}N Relaxation Measurements. The dynamic behavior of the side chain of His149 was investigated using ^1H-detected ^{15}N NMR relaxation measurements. At 30 °C, the T_1 and T_2 lifetimes of the $^{15}N^{\epsilon 2}$ nucleus are 593 ± 12 ms and 74 ± 2 ms, respectively, while the steady-state $^1H-^{15}N$ NOE is 0.67 ± 0.01. When analyzed using the model-free formalism of Lipari and Szabo (30), as described by Farrow et al. (18), these relaxation data correspond to a generalized order parameter S^2 of 0.83 and a chemical shift exchange broadening term, R_{ex}, of 2 s^{-1}. A correlation time of 9.2 ns for the global tumbling of BCX and a contribution due to the CSA for the imidazole nitrogen of 182 ppm were explicitly included in the analysis. The correlation time was determined by a similar investigation of the ^{15}N relaxation rates
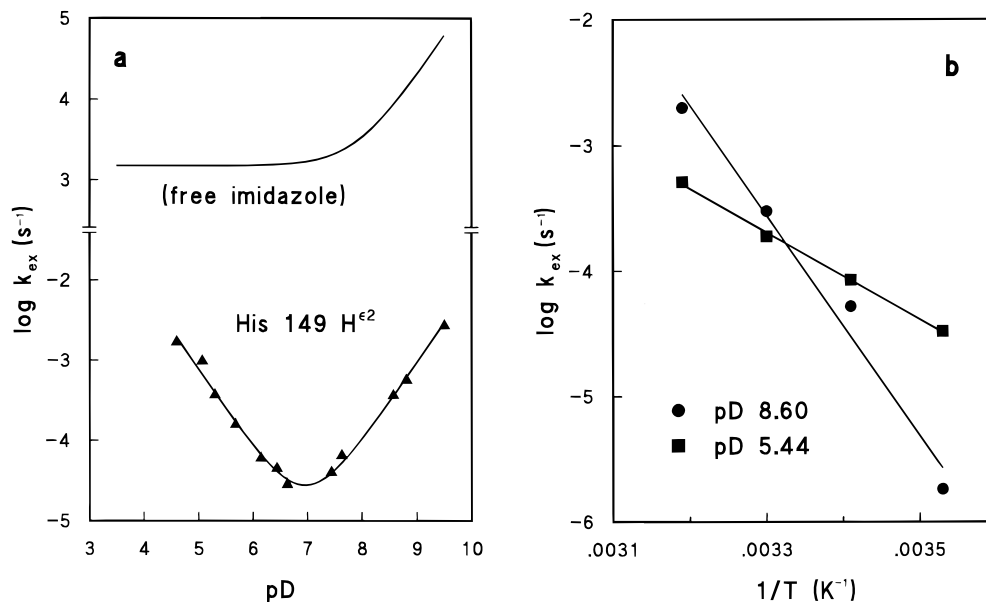
FIGURE 2: (a) Dependence of the observed hydrogen-to-deuterium exchange rate (k_{ex}) of His149 H$^{\epsilon 2}$ in native BCX as a function of pD at 30 °C. The solid line represents the best fit to the equation $k_{ex} = (k_A) 10^{-pD} + (k_B) 10^{(pD - pK_D)} + k_W$, for which the rate constants k_A, k_B, and k_W were determined to be 77 M^{-1} s^{-1}, 470 M^{-1} s^{-1}, and 1.1 × 10^{-5} s^{-1}, respectively. The predicted behavior of k_{ex} versus pD for free imidazole was generated using data previously reported (24, 25). Note the break in the y-axis. (b) Temperature dependence of k_{ex} at pD 5.44 and 8.60, from which the apparent activation energies for exchange by specific acid (7.0 kcal mol^{-1}) and specific base catalysis (17.4 kcal mol^{-1}), respectively, were determined.

of the main-chain amides in the identical protein sample (*17*). The CSA term was calculated from the traceless chemical shift tensor elements reported for the anionic N$^{\epsilon 2}$H tautomer of crystalline histidine (*31*), using expressions for T_1 and T_2 given in Farrow et al. (*18*). In the case of histidine, the chemical shift tensor is not axially symmetric; therefore all three tensor elements were included in the CSA term explicitly.[4] The order parameter S^2 of 0.83 is comparable to those measured for the main-chain amide nitrogens of BCX (G.P.C. and L.P.M., unpublished results). This indicates that the mobility of the imidazole ring of His149 is restricted on the picosecond to nanosecond time scale due to numerous hydrogen-bonding and van der Waals interactions with surrounding residues in the interior of BCX (Figure 1; *5*). The additional R_{ex} term may reflect motions on the microsecond to millisecond time scale, such as conformational averaging, that result in ^{15}N line-broadening. Although it is tempting to speculate that the additional exchange term arises from the exchange of the water to which His149 is hydrogen-bonded, this has not been rigorously explored.

Interactions with a Bound Water and/or Serine Hydroxyl. Inspection of the crystallographic structure of BCX reveals that the H$^{\epsilon 2}$ of His149 is hydrogen-bonded to a buried water molecule, with an O to H$^{\epsilon 2}$ separation of only 1.8 Å (Figure 1). In support of this interaction, a cross-peak was observed between His149 H$^{\epsilon 2}$ and a proton(s) with the chemical shift of bulk water (~4.7 ppm) in the 2D NOESY spectrum of BCX recorded at pH* 5.8 and 30 °C with a gradient 11-echo detection sequence (Figure 5 of ref *15*). Given that the lifetime of His149 H$^{\epsilon 2}$ is 3.5 h under these conditions, this cross-peak cannot arise due to direct chemical exchange

with water. Therefore the cross-peak was attributed to NOE-mediated transfer of magnetization from the bound water and/or the hydroxyl of the nearby Ser100 (O$^{\gamma}$ to H$^{\epsilon 2}$ separation of 3.5 Å). The positive sign of the cross-peak relative to the diagonal corresponds to a negative NOE, indicative of dipolar cross relaxation occurring in the slow-motion regime. We further investigated this using two experimental approaches.

First, we noted that the proton(s) exhibiting the NOESY cross-peak to His149 H$^{\epsilon 2}$ has a chemical shift identical with that of bulk water (*15*). To exclude the possibility that this NOE arises due to a protein proton with a chemical shift coincidentally near 4.7 ppm, NOESY spectra were recorded for BCX in the presence of increasing concentrations of CoCl$_2$. As discussed by Wüthrich and co-workers, the paramagnetic Co^{2+} causes the resonance of bulk water to broaden and move downfield in chemical shift (*22*). The NOESY cross-peak to His149 H$^{\epsilon 2}$ exhibits identical behavior to the bulk water, broadening and moving to 5.0 ppm in the presence of 30 mM CoCl$_2$. This demonstrates that the cross-peak arises from either a proton(s) of the internal water that is in fast exchange on the chemical shift time scale with those of bulk water or the hydroxyl proton of Ser100 that undergoes fast exchange with the aqueous solvent. The upper limit for the bound lifetime of the water or hydroxyl proton(s) is therefore on the order of 10^{-3} s (*22*).

Second, the elegant method of Grzesiek and Bax (*19*) was employed to confirm quantitatively that the NOESY cross-peak arises from a dipolar interaction with a water and/or hydroxyl proton and to exclude further the possibility that the NOE is from a carbon-bonded H$^{\alpha}$ or H$^{\beta}$ proton in BCX with a chemical shift near 4.7 ppm. This method involves selective excitation of the water resonance, with concomitant purging of the signal from any ^{13}C-bonded proton, followed by NOESY- and ROESY-type transfer of magnetization to ^{15}N-bonded protons for detection with a HSQC-based pulse

---

[4] Expressions used for T_1 and T_2 are those given in Farrow et al. (*18*), with the term $(\sigma_{\parallel} - \sigma_{\perp})^2$ in eq 8 being replaced by $[\delta x^2 + \delta y^2 + \delta z^2 - \delta x \delta y - \delta y \delta z - \delta z \delta x]$, where δx, δy, and δz were taken from Munowitz et al. (*31*).
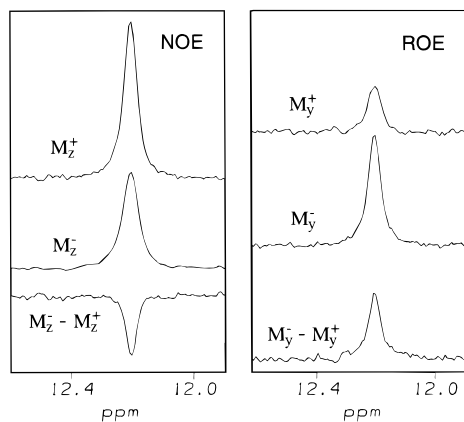
FIGURE 3: A dipolar interaction between His149 $H^{\epsilon 2}$ and a bound water and/or the hydroxyl of Ser100 is detected by a negative NOE and positive ROE. Shown are the spectra of $^{13}C/^{15}N$-labeled BCX recorded with (middle, M^-) and without (top, M^+) selective inversion of the magnetization of water, followed by a 25 ms ROE or 40 ms NOE mixing period and observation of the resulting histidine signal using a 1D HSQC pulse sequence. Difference spectra are shown at the bottom of each panel.

sequence. With mixing times of 40 ms and 25 ms, the normalized ζ_{NOE} and ζ_{ROE} were 0.132 and -0.413, respectively (Figure 3; for a definition of these terms see ref *19*). The relaxation time in the rotating frame, $1/(\rho_2 + k_N) = 17$ ms, was determined by direct measurement of the $T_{1\rho}$ of the $^1H^{\epsilon 2}$ of His149. The relaxation time in the laboratory frame, $1/(\rho_1 + k_N) = 85$ ms, was calculated from the measured $^{15}N^{\epsilon 2}$ $T_1 = 593$ ms and $^{15}N^{\epsilon 2}-^1H^{\epsilon 2}$ $T_{1ZZ} = 74$ ms. From these data, the pseudo-first-order rate constants for exchange of magnetization during the ROE and NOE transfers were determined to be $k_N = 5.3$ s^{-1} and $k_R = -8.7$ s^{-1}, respectively. In the macromolecular or slow-motion limit, pure dipolar cross-relaxation (NOE interaction) will yield a ratio k_R/k_N of -2, whereas exclusive chemical exchange is characterized by k_R/k_N equal to 1. The measured ratio k_R/k_N of ~-1.6 confirms that the observed NOESY cross-peak to His149 $H^{\epsilon 2}$ arises from a NOE-mediated transfer of magnetization from a proton of the bound water molecule and/ or from the hydroxyl of Ser100. Furthermore, the observation of a negative NOE and positive ROE places a lower limit on the lifetime of the water or hydroxyl proton near the overall rotational correlation time of BCX (8.4 ns). Combined with the requirement for fast exchange on the chemical shift time scale, we conclude that the residence time of the bound water proton or Ser100 hydroxyl proton lies between approximately 10^{-8} and 10^{-3} s.

The Grzesiek and Bax (*19*) experiment was also repeated immediately after transfer of ^{15}N-labeled BCX from H_2O to D_2O buffer at pH* 6.5. Whereas the intensity of the signal of His149 $H^{\epsilon 2}$ remained essentially constant, the NOE and ROE interactions with water were completely absent in the first spectra recorded ~8 min after transfer (data not shown). This proves further that the observed NOESY cross-peak to the $H^{\epsilon 2}$ of His149 arises from an exchangeable proton and not a carbon-bonded H^α or H^β with a chemical shift near that of water. Additionally, these experiments demonstrate that the lifetimes of protons from the bound water and/or the hydroxyl of Ser100 in D_2O buffer are significantly shorter than that of the His149 $H^{\epsilon 2}$.

D/H Fractionation Factor. The D/H fractionation factor for the imidazole ring of His149 was determined by measuring the relative intensity of the $H^{\epsilon 2}$ signal as a function of solvent D_2O/H_2O ratio, according to the procedure of Loh and Markley (*23*). The $N^{\epsilon 2}$ of His149 was found to exhibit a slight preference for hydrogen, having a fractionation factor of 0.89 ± 0.02 (data not shown).

Tyrosine Hydrogen-Deuterium Exchange. In addition to the peak from His149 $H^{\epsilon 2}$, two unusually downfield resonances are detected at 11.6 and 12.7 ppm in the ^1H NMR spectrum of BCX (*15*). These remain as singlets when the protein is ^{13}C- and ^{15}N-labeled and thus must arise from protons bonded to O or S atoms. On the basis of their distinct chemical shifts, combined with cross-peaks from the aromatic region of a 2D NOESY spectrum (Figure 5 of ref *15*), we tentatively identify these signals as arising from tyrosine H^η hydroxyl protons. Oxygen-bonded tyrosine protons are rarely detected in the ^1H NMR spectra of proteins (*32−35*), and thus these hydroxyls must be protected from rapid exchange with water due to hydrogen-bonding and/or limited solvent accessibility. Although the resonances from the aromatic rings of the 18 tyrosines in BCX have not been assigned, the most likely candidates are Tyr26, 53, 79, and 105. The hydroxyl groups of these phenyl rings are completely buried within the protein and each participates in at least two possible hydrogen-bonding interactions (*5*).

Hydrogen exchange kinetics of these two putative tyrosine H^η hydroxyl protons were investigated at pD 7.44 and 30 °C. The proton at 11.6 ppm is sufficiently protected that it could be detected after transfer of BCX into D_2O buffer. The measured exchange rate was 0.002 s^{-1}, corresponding to a lifetime of 8 min. In contrast, the proton signal at 12.7 ppm disappeared completely within the time period between solvent transfer and acquisition of the first spectrum. Assuming at least 3 exchange lifetimes occurred during this period of ~8 min, we place a lower boundary on the exchange rate of this hydroxyl proton at 0.006 s^{-1}. In parallel, we estimate an upper limit on its exchange rate at ~1 s^{-1} as this proton is in the regime of slow exchange with water on the chemical shift time scale, and the intensity of its NMR signal does not differ significantly between spectra recorded with and without solvent presaturation (*36*).

DISCUSSION

Kinetic Mechanism of His149 $H^{\epsilon 2}$ Hydrogen Exchange. The classical V-shaped plot of log k_{obs} versus pD with approximately first-order dependence of exchange on [D$^+$] and [OD$^-$] indicates that the $H^{\epsilon 2}$ of His149 exchanges via a bimolecular EX$_2$ mechanism. According to standard formalism, the observed $k_{ex} = P$ k_{int}, where k_{int} is the intrinsic exchange rate of an exposed histidine side chain in an unstructured polypeptide and P is a protection or slowing factor (*26*). P is generally equated to an equilibrium constant for fluctuations between a "closed state" of the protein in which exchange cannot occur and an "open state" in which exchange proceeds at k_{int}. Following this formalism, we propose the schemes for the acid-, base-, and water-catalyzed exchange of the histidine $H^{\epsilon 2}$ in BCX that are shown in Figure 4.

At high pDs, fluctuations of the protein allow abstraction of His149 $H^{\epsilon 2}$ by an OD$^-$ to yield the imidazolate anion. Transfer of a deuteron from D_2O completes the exchange process. The second-order rate constant for base-catalyzed
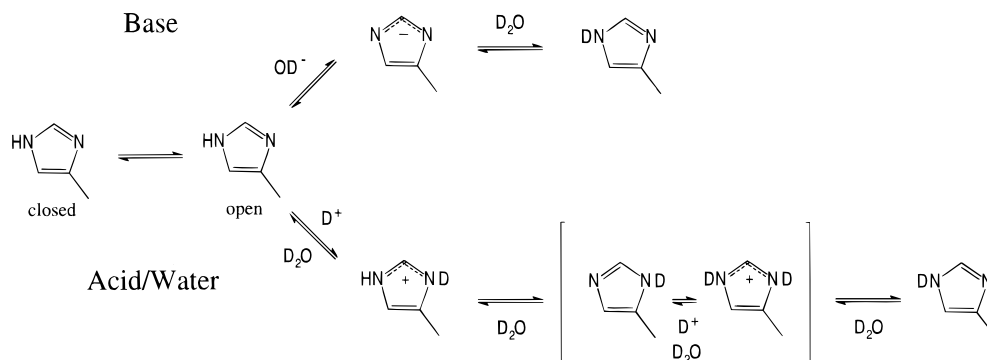
FIGURE 4: Postulated schemes for the base-, acid-, and water-catalyzed exchange of His149 $H^{\epsilon 2}$ in native BCX. Local fluctuations of the protein occur between a "closed state" in which exchange cannot occur and an "open state" in which exchange proceeds at k_{int}. Specific OD^--catalyzed exchange results from the abstraction of the $H^{\epsilon 2}$ to yield the imidazolate anion, followed by rapid transfer of a deuteron from the solvent. Water and specific D^+-catalyzed exchange involves the deuteration of the neutral His149 side chain to yield an imidazolium cation, followed by a series of deuterium transfer steps to regenerate the $N^{\epsilon 2}D$ tautomer.

exchange rate of free imidazole has been reported as 2.3×10^{10} M^{-1} s^{-1} at 25 °C (*25*). This value is consistent with that predicted from the expression $k_{int}/[OD^-] = k_D(\Delta pK_a/(1 + \Delta pK_a))$ where $k_D \sim 10^{10}$ M^{-1} s^{-1} is the second-order diffusion-limited rate constant and $\Delta pK_a = pK_{a(acceptor)} - pK_{a(donor)}$ for the proton-transfer reaction (*26*). Given that the pK_a of $D_2O = 16.4$ at 30 °C (including explicitly the concentration of water as 55.6 M) and that of histidine is 14.4, it is reasonable to predict that the second-order rate constant for the base-catalyzed exchange of histidine in an unstructured polypeptide is similar to that of imidazole, namely, $\sim 10^{10}$ M^{-1} s^{-1} (Figure 2a). Hence, at basic pDs with $k_B = 470$ M^{-1} s^{-1}, we estimate that the protection factor for His149 $H^{\epsilon 2}$ in native BCX is approximately 10^7.

At low pDs, fluctuations of BCX lead to the exchange of the *neutral* imidazole ring of His149. However, for exchange to occur, a cycle such as deuteration of $N^{\delta 1}$, dissociation of $H^{\epsilon 2}$, deuteration of $N^{\epsilon 2}$, and finally dissociation of $D^{\delta 1}$ is required (Figure 4). Assuming that the first deuteration event is rate-limiting and that redistribution of the deuterons is fast (e.g., BCX cannot "refold" with a charged His149), we predict that $k_{ex}/[D^+] \sim 10^{10}$ M^{-1} s^{-1}. This rate constant follows from the assumption of a pK_a of ~ 6.5 for free histidine without distinguishing tautomeric forms and -1.7 for D_3O^+. The calculation also leads to an estimated protection factor of $\sim 10^8$ for the acid-catalyzed exchange of His149, for which $k_A = 77$ M^{-1} s^{-1}. This value agrees well with the protection factor calculated for base-catalyzed exchange, given the approximations involved in estimating k_{int}. A neutral histidine may also abstract a hydrogen directly from water. Assuming a pK_a of ~ 6.5 for histidine and 16.4 for D_2O at 30 °C, the expected rate constant for this pD-independent process is $\sim 10^2$ s^{-1}. Comparison with the measured k_w of 1.1×10^{-5} s^{-1} for His149 also yields a protection factor of $\sim 10^7$. The observed $pD_{min} \sim 7$ for the hydrogen-to-deuterium exchange of His149 $H^{\epsilon 2}$ thus follows from the approximately equal second-order rate constants for the specific acid- and base-catalyzed exchange of the neutral histidine ring, combined with a protection factor that is, to first approximation, pH-independent.

It is instructive to compare the exchange behavior of His149 with that of an exposed imidazole or histidine side chain at acidic pHs. In contrast to the rather unique situation in which His149 is initially neutral in BCX ($pK_a < 2.3$) and thus exhibits specific acid-catalyzed exchange, imidazole is

protonated in solution at pHs less than its pK_a of ~ 6.5. In this situation, exchange is limited by the off rate of the nitrogen-bonded protons due to direct transfer to water. This leads to pH-independent exchange with a reported rate constant of ~ 1500 s^{-1} at 13 °C (Figure 2a; *24*). Due to this fast exchange, nitrogen-bonded protons are normally unobservable in the NMR spectra of an unprotected histidine side chain in water.

General base catalysis of His149 $H^{\epsilon 2}$ exchange is not expected to be significant due to the high pK_a of imidazole versus that of a base such as acetate. However, it is somewhat surprising that general acid-catalyzed exchange was not observed with acetic acid (pK_a 4.7), which should readily transfer a proton to a neutral histidine (pK_a 6.5). For example, at pH 4.7, the predicted exchange rate of a neutral imidazole ring in the presence of 150 mM acetic acid is $\sim 7.5 \times 10^8$ s^{-1}, as compared to 2×10^5 s^{-1} due to H^+ alone. One possible explanation for the lack of such general acid catalysis is limited accessibility of the bulkier acetic acid to His149 in the "open" state compared to H^+ or OH^-. This hypothesis remains to be tested by examining the effects of a series of potential general acid catalysts.

It is interesting to note that one of the candidates for the tyrosines with slowly exchanging hydroxyl protons is Tyr105, the ring of which contacts His149. Based upon an extrapolation of the exchange rates reported for *N*-acetyl-tyrosine methyl ester (*34*), the observed $k_{ex} = 0.002$ s^{-1} for the H^η at 11.6 ppm also corresponds to a protection factor of $\sim 10^6 - 10^7$. It is tempting to speculate that this hydroxyl is indeed from Tyr105 and that exchange proceeds via similar local fluctuations as experienced by His149. However, assignment of the peaks at 11.6 and 12.7 ppm is required to test this suggestion.

Energetics of His149 $H^{\epsilon 2}$ Exchange. When interpreted as an equilibrium constant between "closed" and "open" states, a protection factor of $\sim 10^7$ corresponds to a free energy difference $\Delta G° = -RT \ln P$ of ~ 10 kcal mol^{-1}. Although substantial, this is likely less than $\Delta G°$ for the global, two-state unfolding of BCX at 30 °C, thus indicating that the dominant mechanism of exchange for His149 $H^{\epsilon 2}$ involves more localized fluctuations of the protein. Two arguments support this statement. First, due to irreversible aggregation, the global stability of BCX has not been determined quantitatively. However, an apparent T_m for thermal unfolding of ~ 60 °C (*37*), combined with a $[urea]_{1/2} \sim 5.5$ M at

pH 5.5 and 20 °C (L.P.M., unpublished results), indicates that this protein is indeed stable under the conditions used for these hydrogen exchange measurements. Second, the apparent activation energies for specific acid- and base-catalyzed exchange are 7.0 and 17.4 kcal mol^{-1}, respectively. Consideration of the enthalpy of ionization of water, which leads to a temperature-dependent increase in [OD$^-$] at a given measured pD, reduces the latter value to $\sim$3 kcal mol^{-1}. These activation energies are consistent with small-amplitude local fluctuations of the dynamic ensemble of native structures, allowing exchange to occur within the context of a folded protein. In contrast, they are significantly lower than those expected for exchange processes that are dependent upon the large-amplitude global unfolding of a protein (*26, 38*).

Many of the earliest NMR studies of proteins in H$_2$O solvents focused on "unusually downfield-shifted resonances" attributed to the nitrogen-bonded protons of histidines (*39*). Examples include heme proteins (*40*) and serine proteases (*41−43*), as well as ribonuclease A (*44, 45*), carbonic anhydrase (*46*), and superoxide dismutase (*47*). However, in only a limited number of these cases have the hydrogen exchange kinetics of the histidine residues been investigated. Most notably, Stoesz et al. (*47*) described two histidines in superoxide dismutase with exchange lifetimes of $\sim$11 h at 37 °C and pH 7.2, corresponding to protection factors ($\sim$10^7) comparable to that of His149 in BCX. However, the activation energies for exchange were $\sim$30 kcal mol^{-1}. These value are larger than that observed in the present study but still less than expected for the global unfolding of the protein. Han and Le Mar (*48*) characterized the hydrogen-to-deuterium exchange of the proximal histidines in hemoglobin A. Specific base-catalyzed exchange rate constants of 6−2000 M^{-1} s^{-1} and activation energies of $\sim$25 kcal mol^{-1} were measured at 25 °C, again corresponding to similar exchange lifetimes as observed in the present study. Most recently, Markley and Westler (*49*) reported small protection factors ranging from 1.4 to 9.2 for His 57 in the catalytic triad of bovine chymotrypsin A at 1 °C and pH* 1−9, along with activation free energies of exchange near 12 kcal mol^{-1}. The steeper temperature dependence of histidine exchange in superoxide dismutase and hemoglobin relative to BCX and chymotrypsin may result from the metal ligation of the imidazole groups in the former two proteins.

Structural Environment and Water Interactions. Along with its own amino acid sequence, the conformation of a protein is also affected by water, both as a solvent to be excluded from its hydrophobic interior and as an integral component of its compact, folded structure. In general, proteins contain one or more internal or buried water molecules that provide otherwise missing hydrogen-bond partners and van der Waals contacts to main-chain and side-chain atoms surrounding "cavities" or "packing defects" (*8*). Accordingly, a fundamental goal in biophysics is to understand the role played by these bound waters in establishing the structural, dynamic, and functional properties of proteins.

Inspection of the crystal structure of BCX reveals that His149 is entirely buried within the protein and is involved in an extensive network of hydrogen bonds and van der Waals and aromatic−aromatic interactions (Figure 1). An order parameter S^2 of 0.83, indicative of restricted internal

mobility of the $^{15}N^{\epsilon2}$−H bond vector on the picosecond to nanosecond time scale, is consistent with the highly packed environment of the imidazole side chain. The proximity of its H$^{\epsilon2}$ to a buried water molecule and/or the hydroxyl of Ser100 is supported by a strong dipolar (NOE/ROE) interaction from an oxygen-bonded proton with the chemical shift of bulk water. Using these methods, we cannot unambiguously distinguish whether this NOE arises from a long-lived water (nanosecond to millisecond residence time) or a serine hydroxyl that is in fast exchange (τ_{ex} less than milliseconds) with the pool of solvent molecules. However, two arguments support strongly the presence of a bound water, hydrogen-bonded to His149 H$^{\epsilon2}$, in solution as well as in the crystalline state.

First, the rate constants for NOE and ROE transfers are given by the expressions $k_N = d[6J(2\omega) - J(0)]$ and $k_R = d[3J(\omega) + 2J(0)]$, where $d = (^1/_{10})(h\gamma^2/r^3)^2$ (*50*). In the simplest model of a rigidly bound water molecule (or side-chain hydroxyl), the spectral density function can be written as $J(\omega) = \tau_c/[1 + (\tau_c\omega)^2]$. Using a global correlation time τ_c of 9.2 ns for BCX and our measured values of k_N and k_R, we calculate a separation, r, of 2.2 or 2.5 Å between His149 H$^{\epsilon2}$ and a single proton or two equidistant protons, respectively. Inclusion of possible internal motion of the water or hydroxyl would require an even shorter separation. Based on the crystal structure of BCX, His149 H$^{\epsilon2}$ is $\sim$2.3 and 2.4 Å from the expected positions of the protons on the bound water and $\sim$3.2 Å from the hydroxyl proton of Ser100 (Figure 1). Therefore, it is very likely that the internal water molecule is the dominant source of the NOE interaction with His149 H$^{\epsilon2}$, though a small contribution from Ser100 may also be present.

Second, whereas His149, Tyr105, and Ser130 are absolutely conserved in all family G xylanases, Asp101 may be substituted by Asn and Ser100 by Cys, Ala, and Val (using residue numbering corresponding to BCX; *3*). Furthermore, the interaction between His149, Asp101, and Tyr105 and the bound water, as illustrated in Figure 1 for BCX, is also observed in the crystal structures of the related *Trichoderma harzianum, Trichoderma reesei* I and II, and *Thermomyces lanuginosus* xylanases (*3, 5, 12−14*). However, in the latter protein, a disulfide bond exists to position 100, indicating that Ser100 is not absolutely required for binding of the water molecule. A thermally stable version of BCX with a similar disulfide bond to position 100 has also been characterized (*4*). These patterns of sequence and structural conservation suggest strongly that a tightly bound water forms an integral part of the native fold of these xylanases and that this long-lived water is indeed hydrogen-bonded to His149 in solution.

Although controversial (see refs *51* and *52*), the equilibrium preference of a nitrogen or oxygen in a protein to bond to deuterium versus hydrogen relative to that exhibited by the oxygen of bulk water has been interpreted in terms of strong hydrogen-bonding interactions (*23, 53−55*). Histidine protons involved in these so-called low-barrier hydrogen bonds (LBHBs) typically exhibit anomolously small fractionation factors ($\sim$0.5) and strongly downfield-shifted NMR signals ($\sim$18 ppm) (*49*). To investigate the nature of the hydrogen bond between the bound water and His149, we measured the D/H fractionation factor of this side chain. The N$^{\epsilon2}$ of His149 exhibits a small preference for hydrogen, with a D/H fractionation factor of 0.89 $\pm$ 0.02. Although the

reference value for free histidine or imidazole has not been reported, that of the amide group is ~1.2 (*56*). Therefore, hydrogen bonding of His149 $N^{\epsilon 2}$ to the bound water molecule may slightly reduce the D/H fractionation factor of this side chain. However, the fact that the chemical shift of His149 is 12.2 ppm rather than ~18 ppm as seen for other histidines postulated to be involved in LBHBs (*49*, *54*), argues that this bond is not "unusually" strong. In addition, LBHBs described in the literature for histidines in proteins are intramolecular and not to buried water molecules.

The lifetimes of the protons on the bound water that is hydrogen-bonded to His149 in BCX are within the range of $10^{-8}-10^{-3}$ s. This range, typical of tightly bound waters in proteins (*57*, *58*), was determined by the observation of a strong negative NOE to the histidine side chain and chemical shifts equal to that of bulk solvent. Therefore, at neutral pH, these protons exchange with solvent ~10^7-10^{13} fold faster than does His149 $H^{\epsilon 2}$. Two possible mechanisms can be envisioned for exchange of water protons. In the first, transfer of protons to the bound water oxygen occurs "chemically" via specific acid and base catalysis, whereas in the second, exchange follows from the "physical" replacement of the entire water molecule by diffusion with an equivalent molecule from the solvent pool. We cannot distinguish these possibilities on the basis of the experiments reported in this study. However, ^{17}O and ^2H magnetic relaxation dispersion measurements have shown that the lifetimes of the four buried water molecules (including the oxygens) in BPTI fall within the range of $10^{-8}-10^{-4}$ s (*59*). By inference, this suggests strongly that the entire water molecule in BCX, and not just its protons, undergoes rapid exchange with the solvent on a nano- to millisecond time scale.

Following this argument, we conclude that the hydrogen bond between His149 $H^{\epsilon 2}$ and the buried water molecule must also be broken on a time scale of $10^{-8}-10^{-3}$ s to allow replacement of the latter with a solvent molecule. The 10^7-fold protection from H–D exchange observed for His149 can be attributed to this interaction, provided the hydrogen bond re-forms with the exchanging water faster than k_{int} for the imidazole proton (EX$_2$ regime; *26*). However, it is likely that the hydrophobic environment of the histidine ring within the folded interior of BCX also contributes to the retarded exchange kinetics of His149 $H^{\epsilon 2}$. Local fluctuations of the protein may be required to extensively expose the side chain of this residue to the solvent, allowing base-catalyzed deprotonation to yield a negatively charged imidazolate or acid-catalyzed protonation of *both* $N^{\epsilon 2}$ and $N^{\delta 1}$ to produce the positively charged imidazolium group (Figure 4). Because the pK_a of His149 in native BCX is <2.3, local refolding will occur only after re-formation of the neutral imidazole ring. Given the relative time scales of these events, the fluctuations leading to the exposure of His149 are likely to be more extensive that those required to allow transfer of water molecules between the solvent and protein interior. It is interesting to note that a LBHB has been proposed to exist in the catalytic triad of chymotrypsinogen on the basis of a fractionation factor of ~0.4 and a histidine chemical shift of 18.1 ppm (*49*). However, an exchange protection factor of only 9.2 argues that a "strong" hydrogen bond alone does not prevent exchange of this histidine proton with the solvent.

In conclusion, His149 clearly plays an important structural role in BCX, as evidenced by its extremely low pK_a and its evolutionary conservation. We have examined the dynamic properties of the side chain of this distinctive residue and its interaction with a buried water using experimental techniques that are sensitive to motions in three different time regimes. ^{15}N relaxation experiments show that its imidazole ring is held rigidly within the protein on a pico- to nanosecond time scale. Although entirely buried, HX studies reveal that local fluctuations of BCX allow the $H^{\epsilon 2}$ of His149 to exchange with the solvent on the time scale of hours. This protection from exchange must result from the location of the histidine in the core of the protein and/or its involvement in a network of hydrogen bonds. However, NOE and chemical shift measurements demonstrate that the lifetime of the hydrogen-bonding internal water is on the order of $10^{-8}-10^{-3}$ s. This is indicative of small-scale fluctuations that allow its diffusion to the bulk solvent yet preclude the acid- and base-catalyzed exchange of the imidazole proton of His149. Together, these studies illustrate the range of dynamic behavior possible for a single side chain within the context of a folded protein molecule.

ACKNOWLEDGMENT

REFERENCES

1. Glasoe, P. F., and Long, F. A. (1960) *J. Phys. Chem. 64*, 188–193.
2. Wakarchuk, W. W., Methot, N., Lanthier, P., Sung, W., Seligy, V., Yaguchi, M., To, R., Campbell, R., and Rose, D. (1992) in *Xylan and Xylanases* (Visser, J. V., et al., Eds.) pp 439–442, Elsevier Science B. V., Amsterdam.
3. Wakarchuk, W. W., Campbell, R. L., Sung, W. L., Davoodi, J., and Yaguchi, M. (1994) *Protein Sci. 3*, 467–475.
4. Wakarchuk, W. W., Sung, W. L., Campbell, R. L., Cunningham, A., Watson, D. C., and Yaguchi, M. (1994) *Protein Eng. 7*, 1379–1386.
5. Campbell, R., Rose, D., Wakarchuk, W. W., To, R., Sung, W., and Yaguchi, M. (1993) in *Proceedings of the Second TRICEL Symposium on Trichoderma reesei* Cellulases and Other Hydrolases (Suominen, P., & Reinikainen, T., Eds.) pp 63–77, Foundation for Biotechnical and Industrial Fermentation Research, Helsinki, Finland.
6. Miao, S., Ziser, L., Aebersold, R., and Withers, S. G. (1994) *Biochemistry 33*, 7027–7032.
7. McIntosh, L. P., Hand, G., Johnson, P. E., Joshi, M. D., Korner, M., Plesniak, L. A., Ziser, L., Wakarchuk, W. W., and Withers, S. G. (1996) *Biochemistry 35*, 9958–9966.
8. Williams, M. A., Goodfellow, J. M., and Thornton, J. M. (1994) *Protein Sci. 3*, 1224–1235.
9. Evans, S. (1993) *J. Mol. Graphics 11*, 134–138.
10. Gilkes, N. R., Henrissat, B., Kilburn, D. G., Miller, R. C., Jr., and Warren, R. A. J. (1991) *Microbiol. Rev. 55*, 303–315.
11. Henrissat, B., and Bairoch, A. (1993) *Biochem. J. 293*, 781–788.
12. Törrönen, A., Harkki, A., and Rouvinen, J. (1994) *EMBO J. 13*, 2943–2501.
13. Törrönen, A., and Rouvinen, J. (1995) *Biochemistry 34*, 847–856.
14. Schacher, R. A., Holzman, K., Hayn, M., Steiner, W., and Schwab, H. (1996) *J. Biotechnol. 49*, 211–218.
15. Plesniak, L. A., Connelly, G. P., Wakarchuk, W. W., and McIntosh, L. P. (1996) *Protein Sci. 5*, 2319–2328.

16. Sung, W. L., Luk, C. K., Zahab, D. M., and Wakarchuk, W. W. (1993) *Protein Expression Purif. 4*, 200−216.

17. Plesniak, L. A., Wakarchuk, W. W., and McIntosh, L. P. (1996) *Protein Sci. 5*, 1118−1135.

18. Farrow, N. A., Muhandiram, R., Singer, A. U., Pascal, S. M., Kay, C. M., Gish, G., Shoelson, S. E., Pawson, T., Forman-Kay, J. D., and Kay, L. E. (1994) *Biochemistry 33*, 5984−6003.

19. Grzesiek, S., and Bax, A. (1993) *J. Biomol. NMR 3*, 627−638.

20. Pascal, S. M., Yamazaki, T., Singer, A. U., Kay, L. E., and Forman-Kay, J. D. (1995) *Biochemistry 34*, 11353−11362.

21. Sklenár, V., and Bax, A. (1987) *J. Magn. Reson. 74*, 469−479.

22. Otting, G., Liepinsh, E., and Wüthrich, K. (1991) *J. Am. Chem. Soc. 113*, 4363−4364.

23. Loh, S. N., and Markley, J. L. (1993) *Tech. Protein Chem. 4*, 517−524.

24. Eigen, M., Hammes, G. G., and Kustin, K. (1960) *J. Am. Chem. Soc. 82*, 3482−3483.

25. Eigen, M., and Hammes, G. G. (1963) *Adv. Enzymol. Relat. Subj. Biochem. 25*, 1−38.

26. Englander, S. W., and Kallenbach, N. R. (1984) *Q. Rev. Biophys. 16*, 521−655.

27. Bai, Y., Milne, J. S., Mayne, L., and Englander, S. W. (1993) *Proteins: Struct., Funct., Genet. 17*, 75−86.

28. Covington, A. K., Robinson, R. A., and Bates, R. G. (1966) *J. Phys. Chem. 70*, 3820−3824.

29. Kim, P. S., and Baldwin, R. L. (1982) *Biochemistry 21*, 1−5.

30. Lipari, G., and Szabo, A. (1982) *J. Am. Chem. Soc. 104*, 4546−4559.

31. Munowitz, M., Bachovchin, W. W., Herzfeld, J., Dobson, C. M., and Griffin, R. G. (1982) *J. Am. Chem. Soc. 104*, 1192−1196.

32. Kraulis, P. J., Clore, G. M., Nilges, M., Jones, T. A., Petterson, G., Knowles, J., and Gronenborn, A. M. (1989) *Biochemistry 28*, 7241−7257.

33. Torchia, D. A., Sparks, S. W., and Bax, A. (1989) *Biochemistry 28*, 5509−5524.

34. Liepinsh, E., Otting, G., and Wüthrich, K. (1992) *J. Biomol. NMR 2*, 447−465.

35. Mollova, E. T., Metzler, D. E., Kintanar, A., Kagamiyama, H., Hayashi, H., Hirotsu, K., and Miyahara, I. (1987) *Biochemistry 26*, 615−625.

36. Sandström, J. (1982) in *Dynamic NMR Spectroscopy*, Academic Press, New York.

37. Davoodi, J., Wakarchuk, W. W., Campbell, R. L., Carey, P. R., and Surewicz, W. K. (1995) *Eur. J. Biochem. 232*, 839−843.

38. Woodward, C. K., Simon, I., and Tüchsen, E. (1982) *Mol. Cell. Biochem. 48*, 135−160.

39. Markley, J. L. (1975) *Acc. Chem. Res. 8*, 70−80.

40. Redfield, A. G., and Gupta, R. K. (1971) *J. Chem. Phys. 54*, 1418−1419.

41. Robillard, G., and Schulman, R. G. (1974) *J. Mol. Biol. 86*, 519−540.

42. Markley, J. L. (1978) *Biochemistry 22*, 4648−4656.

43. Bachovchin, W. W. (1985) *Proc. Natl. Acad. Sci. U.S.A. 82*, 7948−7951.

44. Griffin, J. H., Cohen, J. S., and Schechter, A. N. (1973) *Biochemistry 12*, 2096−2099.

45. Patel, D. J., Woodward, C. K., and Bovey, F. A. (1972) *Proc. Natl. Acad. Sci. U.S.A. 69*, 599−602.

46. Gupta, R. K., and Pesando, J. M. (1975) *J. Biol. Chem. 250*, 2630−2634.

47. Stoesz, J. D., Malinowski, D. P., and Redfield, A. G. (1979) *Biochemistry 18*, 4669−4675.

48. Han, K.-H., and LeMar, G. N. (1986) *J. Mol. Biol. 189*, 541−552.

49. Markley, J. L., and Westler, W. M. (1996) *Biochemistry 35*, 11092−11097.

50. Wang, Y.-X., Freedberg, D. I., Grzesiek, S., Torchia, D. A., Wingfield, P. T., Kaufman, J. D., Stahl, S. J., Chang, C.-H., and Hodge, C. N. (1996) *Biochemistry 35*, 12694−12704.

51. LiWang, A. C., and Bax, A. (1996) *J. Am. Chem. Soc. 118*, 12864−12865.

52. Gerlt, J. A., Kreevoy, M. M., Cleland, W. W., and Frey, P. A. (1997) *Chem. Biol. 4*, 259−267.

53. Bowers, P. M., and Klevit, R. E. (1996) *Nat. Struct. Biol. 3*, 522−531.

54. Halkides, C. J., Wu, Y. Q., and Murray, C. J. (1996) *Biochemistry 35*, 15941−15948.

55. Smirnov, S. N., Golubev, N. S., Denisov, G. S., Benedict, H., Schah-Mohammedi, P., and Limbach, H.-H. (1996) *J. Am. Chem. Soc. 118*, 4094−4101.

56. Englander, S. W., and Poulsen, A. (1969) *Biopolymers 7*, 379−393.

57. Gerothanassis, I. P. (1994) *Prog. NMR Spectrosc. 26*, 171−237.

58. Billeter, M. (1995) *Prog. NMR Spectrosc. 27*, 635−645.

59. Denisov, V. P., Peters, J., Hörlein, H. D., and Halle, B. (1996) *Nat. Struct. Biol. 3*, 505−509.